Nonlinear Radar via Intermodulation of FM Noise Waveform Pairs

Jonathan Owen[1], Shannon D. Blunt[1], Kyle Gallagher[2], Patrick McCormick[1], Christopher Allen[1], Kelly Sherbondy[2]
[1] Radar Systems Lab (RSL), University of Kansas, Lawrence, KS
[2] Sensors and Electron Devices Division, Army Research Laboratory (ARL), Adelphi, MD

***Abstract*— To take advantage of the unique scattering responses associated with nonlinear radar, the predominant approach involves the detection of target-induced harmonics elicited by the interrogation of a single spectrally pure waveform (often a tone). In contrast, we consider the impact of using a pair of high-dimensional waveforms to realize a novel nonlinear intermodulation approach. The interrogating waveforms in this case are two unique sets of FM noise waveforms that also permit the high incident power necessary to induce a nonlinear response. Both waveforms reside in the resonant region of the device under test, with their intermodulated response signal made sufficiently separable from the second-order harmonics of each individual waveform in the same band by virtue of very high dimensionality. This framework, collectively denoted as shared-spectrum pseudo-random intermodulation (SSPRInt), is demonstrated via simulation and experimentally in a loopback configuration.**

Keywords—nonlinear radar, waveform diversity, FM noise

I. Introduction

The general concept of nonlinear radar has been known since the 1970s (see [1]) and has been employed for a variety of purposes including animal tracking, temperature sensing, and monitoring of human vital signs (e.g. [2-4]). Nonlinear radar relies on the phenomenological attribute of certain scatterers, including RF electronics such as cellular telephones and radios, to produce a measurable response at a frequency that is discernible from that of the interrogating signal. The resulting frequency offset therefore permits the possible detection and discrimination of these particular responses against the backdrop of linear clutter echoes received at a much higher power. It has even been observed that dolphins exploit a form of linear/nonlinear discrimination with biosonar in bubble-rich environments [5] and their approach has likewise been recently mimicked for radar applications [6].

A recent survey of research on nonlinear radar [7] provides an overview of the myriad approaches and applications that have been explored in this context and also establishes the design trade-space and best practices. Specifically, it is noted in [7] that "*researchers working on nonlinear radar have overwhelmingly chosen to exploit the harmonic responses of targets rather than intermodulation.*" For transmitted frequency f_0, the prevalent class of nonlinear radar denoted as harmonic radar seeks to detect the presence of harmonics $2f_0$, $3f_0$, etc. within the resulting reflections. For this detection to be meaningful, it is clearly necessary to suppress any such harmonics from being self-generated by the transmitter, thus placing strict requirements on spectral purity [8].

In contrast, a much smaller subset of nonlinear radar research has relied on the intermodulation of different signals (see [9,10] and references therein). For example, frequencies f_1 and f_2 would produce intermodulation frequencies f_1+f_2, f_1-f_2, $2f_1+f_2$, $2f_1-f_2$, and so on that are distinct from the individual harmonics (e.g. $2f_1$ and $2f_2$ for second harmonics). However, because RF devices generally contain a front-end bandpass filter [10,11] (see Fig. 1), the bandwidth over which a nonlinear response can be elicited is limited. Consequently, intermodulation signals tend to still be relatively near in frequency to the harmonics, thus precluding easy separation.

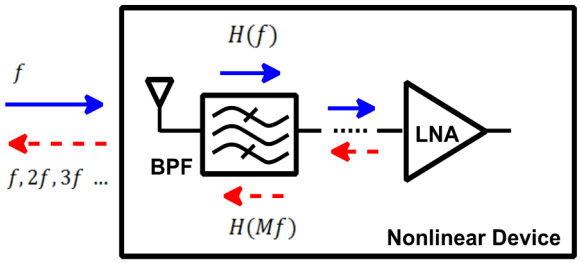

Fig. 1: Standard model of a nonlinear device (from [10,11]) consisting of an antenna, a bandpass filter, and a nonlinear component (here a low-noise amplifier)

Here we propose a waveform diversity [12,13] based approach to intermodulation radar that leverages a recently demonstrated form of FM noise [14,15] denoted as pseudo-random optimized (PRO) FM. The relevant benefits of this manner of waveform are *a*) it can be generated in a pulsed form at high power so as to elicit a nonlinear response and *b*) it can achieve tremendously high time-bandwidth products because it never repeats ($BT > 10^7$ has been experimentally demonstrated). This latter property is the key facilitator to the realization of intermodulation responses that are highly separable from the individual harmonic signals. The effect is accomplished by the emission of large sets of unique pairs of PRO-FM waveforms followed by coherent integration across the set of intermodulated waveform responses on receive. This separation capability is demonstrated in simulation and experimentally in loopback.

II. Intermodulation & Harmonic Waveforms

The second harmonic is most commonly used for nonlinear radar because the nonlinear reflected power decreases exponentially with the order of the harmonic [16]. If we were to generate simple sinusoidal tones at frequencies f_1 and f_2, the resulting second-order signals of interest are the individual harmonics $2f_1$ and $2f_2$, and the intermodulation term f_1+f_2. Per Fig. 1, the presence of the bandpass filter in any nonlinear device that we may wish to detect limits the separability of

This work was supported by the Army Research Office under Contract # W911NF-15-2-0063.

these signals in frequency, particularly because the linear scattering is received with orders-of-magnitude higher power.

More generally, now consider two arbitrary waveforms

$$s_1(t) = \cos\big(2\pi f_C t + \phi_1(t)\big)$$
$$s_2(t) = \cos\big(2\pi f_C t + \phi_2(t)\big) \quad (1)$$

where $\phi_1(t)$ and $\phi_2(t)$ are the respective continuous phase functions and f_C is the center frequency. We shall assume that both waveforms possess the same 3-dB bandwidth. These and all subsequent waveforms/signals are summarized in Table I for easy reference.

The waveforms are produced by separate transmitters and we wish to detect their intermodulation product in the nonlinear radar receiver. Because these waveforms must be generated at sufficiently high power, harmonics are produced by each transmitter that can be represented in the form of a power series [17-19]. In particular, the second-order harmonics of the waveforms in (1) can be expressed as

$$\begin{aligned} s_1^2(t) &= \cos^2\big(2\pi f_C t + \phi_1(t)\big) \\ &= 0.5\big\{1 + \cos\big(4\pi f_C t + 2\phi_1(t)\big)\big\} \\ &= 0.5 + 0.5 s_{11}(t) \end{aligned} \quad (2)$$

and

$$\begin{aligned} s_2^2(t) &= \cos^2\big(2\pi f_C t + \phi_2(t)\big) \\ &= 0.5\big\{1 + \cos\big(4\pi f_C t + 2\phi_2(t)\big)\big\} \\ &= 0.5 + 0.5 s_{22}(t), \end{aligned} \quad (3)$$

for $s_{11}(t)$ and $s_{22}(t)$ the harmonic waveforms arising from the original waveforms individually. Note that these harmonic waveforms possess twice the bandwidth as their fundamental counterparts and also reside at twice the center frequency.

TABLE I. SIGNAL DESCRIPTIONS FOR SSPRINT NONLINEAR RADAR

Signal	*Description*
$s_1(t)$	Transmitted waveform 1 at f_C
$s_2(t)$	Transmitted waveform 2 at f_C
$s_{11}(t)$	Harmonic waveform 1 at $2f_C$
$s_{22}(t)$	Harmonic waveform 2 at $2f_C$
$s_{12}(t)$	Intermodulation waveform at $2f_C$
$r_{12}(t)$	Autocorrelation of $s_{12}(t)$
$c_{12,11}(t)$	Cross-correlation between $s_{12}(t)$ and $s_{11}(t)$
$c_{12,22}(t)$	Cross-correlation between $s_{12}(t)$ and $s_{22}(t)$
$s_{11,m}(t)$	Harmonic waveform 1 at $2f_C$, *m*th pulse
$s_{22,m}(t)$	Harmonic waveform 2 at $2f_C$, *m*th pulse
$s_{12,m}(t)$	Intermodulation waveform at $2f_C$, *m*th pulse
$\bar{r}_{12}(t)$	Coherent autocorrelation averaged over *M* pulses
$\bar{c}_{12,11}(t)$	Coherent cross-correlation averaged over *M* pulses
$\bar{c}_{12,22}(t)$	Coherent cross-correlation averaged over *M* pulses

The intermodulation can likewise be expressed as the power series operation [17-19] on the superposition of the two waveforms in (1), which can be written as

$$\begin{aligned} &\big(s_1(t) + s_2(t)\big)^2 \\ &\quad = \big(\cos\big(2\pi f_C t + \phi_1(t)\big) + \cos\big(2\pi f_C t + \phi_2(t)\big)\big)^2 \\ &\quad = \cos^2\big(2\pi f_C t + \phi_1(t)\big) + \cos^2\big(2\pi f_C t + \phi_2(t)\big) \\ &\qquad + 2\cos\big(2\pi f_C t + \phi_1(t)\big) \cdot \cos\big(2\pi f_C t + \phi_2(t)\big) \\ &\quad = 0.5\big\{1 + \cos\big(4\pi f_C t + 2\phi_1(t)\big)\big\} \\ &\qquad + 0.5\big\{1 + \cos\big(4\pi f_C t + 2\phi_2(t)\big)\big\} \\ &\qquad + \cos\big(\phi_1(t) - \phi_2(t)\big) \\ &\qquad + \cos\big(4\pi f_C t + \phi_1(t) + \phi_2(t)\big) \\ &\quad = 1 + 0.5 s_{11}(t) + 0.5 s_{22}(t) + s_{1-2}(t) + s_{12}(t). \end{aligned} \quad (4)$$

At the bottom of (4), the $s_{11}(t)$ and $s_{22}(t)$ terms are the second-harmonic waveforms from (2) and (3). The $s_{1-2}(t)$ term is the mixing product translated to baseband that does not propagate, so we shall ignore it.

The final term in (4) is the intermodulation waveform $s_{12}(t)$ that should only be produced by nonlinear scattering in the environment given adequate isolation between the two transmitters and neglecting intermodulation effects within the radar receiver. This waveform resides in the same spectral footprint (same bandwidth and center frequency) as the two harmonic waveforms. Thus their separability is completely dictated by the respective cross-correlations

$$c_{12,11}(t) = \int \tilde{s}_{12}^*(t)\, \tilde{s}_{11}(t+\tau) d\tau$$
$$c_{12,22}(t) = \int \tilde{s}_{12}^*(t)\, \tilde{s}_{22}(t+\tau) d\tau, \quad (5)$$

where $\tilde{s}_{12}(t)$, $\tilde{s}_{11}(t)$, and $\tilde{s}_{22}(t)$ are the complex baseband versions of these waveforms. In contrast, the correlation of $\tilde{s}_{12}(t)$ with itself, i.e. a matched filtering process, produces the autocorrelation response

$$r_{12}(t) = \int \tilde{s}_{12}^*(t)\, \tilde{s}_{12}(t+\tau) d\tau \quad (6)$$

that possesses a discernible mainlobe and sidelobes on the order of $-10\log_{10}(BT)$.

Therefore the crux of the problem lies in how to obtain waveforms $s_1(t)$ and $s_2(t)$ such that the cross-correlations in (5) and sidelobes in (6) are minimized. It is important to note that the relationship between the cross-correlation and the cross-spectrum via the Wiener-Khintchine theorem effectively places a lower bound on how small the cross-correlations in (5) can be since $\tilde{s}_{11}(t)$, $\tilde{s}_{22}(t)$, and $\tilde{s}_{12}(t)$ all occupy the same spectrum and have constant envelopes. Given the bandwidth restriction imposed by a hypothetical bandpass filter from Fig. 1 and the achievable pulsewidth for which high power can be achieved, along with the expectation of linear scattering from the versions of $s_{11}(t)$ and $s_{22}(t)$ unintentionally generated by the transmitter, it consequently stands to reason that it may not be feasible to obtain a single pair of waveforms $s_1(t)$ and $s_2(t)$ that achieve a sufficient degree of separability for (5).

To address this problem we propose to use multiple unique pairs of FM noise waveforms that can be written as the simple generalization of (1) as

$$s_{1,m}(t) = \cos\left(2\pi f_C t + \phi_{1,m}(t)\right)$$
$$s_{2,m}(t) = \cos\left(2\pi f_C t + \phi_{2,m}(t)\right) \quad (7)$$

for the *m*th of *M* pulses. By extension, the *m*th set of harmonic waveforms and the *m*th intermodulation waveform respectively become $s_{11,m}(t)$, $s_{22,m}(t)$, and $s_{12,m}(t)$.

While any given pair of the waveforms in (7) can be no better than those in (1), the coherent combining of *M* intermodulated responses of $s_{12,m}(t)$ after individual matched filtering like in (6) provides an effective time-bandwidth product that is *M* times greater than a single waveform. As such, the coherently averaged autocorrelation becomes

$$\bar{r}_{12}(t) = \frac{1}{M}\sum_{m=1}^{M}\int \tilde{s}^{*}_{12,m}(t)\,\tilde{s}_{12,m}(t+\tau)d\tau\,, \quad (8)$$

for which the mainlobe is unchanged but the sidelobes are reduced by roughly a factor of *M* due to their combining incoherently [14,15]. Further, the cross-correlation responses from (5) likewise combine incoherently, resulting in

$$\bar{c}_{12,11}(t) = \sum_{m=1}^{M}\int \tilde{s}^{*}_{12,m}(t)\,\tilde{s}_{11,m}(t+\tau)d\tau \approx \frac{1}{M}\,c_{12,11}(t) \quad (9)$$

and

$$\bar{c}_{12,22}(t) = \sum_{m=1}^{M}\int \tilde{s}^{*}_{12,m}(t)\,\tilde{s}_{22,m}(t+\tau)d\tau \approx \frac{1}{M}\,c_{12,22}(t), \quad (10)$$

which again is roughly a factor of *M* reduction relative to (5).

III. FM Noise Waveforms

The concept of FM noise waveforms was theoretically analyzed in [20-22] and a practical form using spectral shaping via alternating projections optimization was experimentally demonstrated in [14,15]. Since then, such waveforms have demonstrated a capability for practical spectral notching on transmit [23-27], a means to facilitate advanced emission structures involving polarization and spatial modulation [28,29], and gradient-based optimization approaches have also been realized [30,31]. Here we briefly summarize the alternating projections version denoted as pseudo-random optimized (PRO) FM that serves as the basis for this nonlinear radar formulation.

Given a desired power spectrum $|G(f)|^2$, here selected to be Gaussian due to the associated Gaussian autocorrelation, and an initial randomized FM waveform $s_{1,m,0}(t)$ obtained using a random instantiation of the polyphase-coded FM (PCFM) implementation [32], the projections [15]

$$r_{1,m,k+1}(t) = \mathcal{F}^{-1}\{|G(f)|\exp(j\angle\mathcal{F}\{s_{1,m,k}(t)\})\} \quad (11)$$
$$s_{1,m,k+1}(t) = \exp\left(j\angle r_{1,m,k+1}(t)\right) \quad (12)$$

are applied *K* times in alternating fashion. The operation $\angle(\bullet)$ in (11) and (12) extracts the phase of the argument, while $\mathcal{F}\{\bullet\}$ and $\mathcal{F}^{-1}\{\bullet\}$ are the Fourier transform and inverse Fourier transform, respectively. The first stage (11) enforces the spectrum shape and the second (12) enforces a constant amplitude pulse.

After *K* iterations of (11) and (12) the final waveform is denoted as $s_{1,m}(t)$. The same process is repeated using an independent initialization to obtain $s_{2,m}(t)$. The independent initializations result in unique waveforms after the alternating projections procedure, thereby providing the benefit of incoherent combining of autocorrelation and cross-correlation sidelobes that serve to decorrelate the intermodulation response from the harmonic responses. This high-dimensional decorrelation capability is what enables the needed separability without resorting to complicated transmitter linearization methods.

IV. Simulated and Experimental Results

First consider the properties of an intermodulation waveform $s_{12}(t)$ produced from a pair of FM noise waveforms that are generated using the PRO-FM formulation, as well as the relationship $s_{12}(t)$ has with the two harmonic waveforms $s_{11}(t)$ and $s_{22}(t)$. Two waveforms are generated that each have a time-bandwidth product of $BT = 50$, defined according to 3-dB bandwidth. The associated harmonic and intermodulation waveforms thus have $BT = 100$.

Figure 2 illustrates the autocorrelation function (ACF) of a single $s_{12}(t)$ intermodulation waveform as well as the cross-correlation functions (CCFs) from (5). While one could most likely optimize two waveforms to achieve better cross-correlation than what is observed here, the time-bandwidth product of 100 implies that the best that could be achieved is a separability on the order of about −20 dB [12]. Also note that this result does not account for the relative scaling of the harmonic and intermodulation responses, where the former would otherwise tend to mask the latter due to the linear scattering induced by unintentionally generated versions of the harmonic waveforms by the separate transmitters.

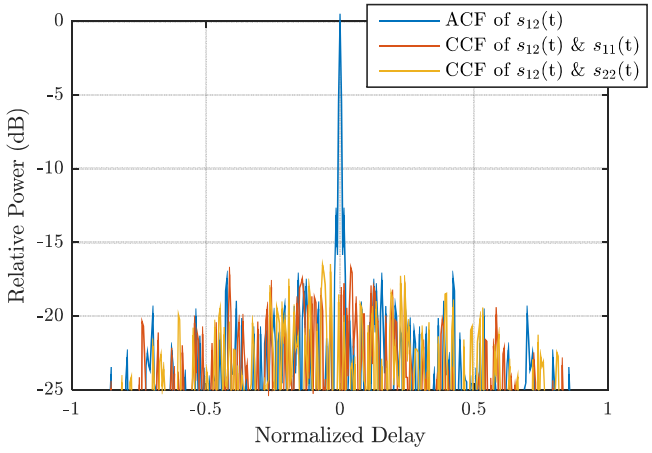

Fig. 2: Simulated correlations between the modeled intermodulation $s_{12}(t)$ and harmonics $s_{11}(t)$ & $s_{22}(t)$ for a single pulse

However, when 100,000 unique PRO-FM pulse pairs are produced, the coherently integrated ACF from (8) and the coherently integrated CCFs from (9) and (10) are realized. Specifically, it is observed that the cross-correlation responses have been reduced by around 50 dB, which is in line with the incoherent sidelobe suppression of 10 $\log_{10}(100{,}000) = 50$ dB. Thus there is good reason to believe that shared-spectrum pseudo-random intermodulation (SSPRInt) can perform as intended, particularly when the intermodulation response is masked by the harmonic responses.

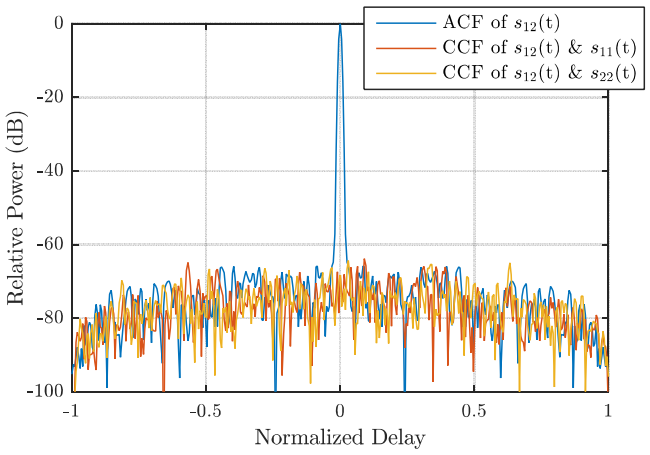

Fig. 3: Simulated averaged correlations between the modeled intermodulation $s_{12}(t)$ and harmonics $s_{11}(t)$ & $s_{22}(t)$ for 100,000 unique PRO-FM pulse pairs

We now evaluate SSPRInt from an experimental perspective. The same two sets of 100,000 PRO-FM waveform pairs were simultaneously transmitted using separate channels of a Tektronix AWG70002A arbitrary waveform generator (AWG) at a center frequency of 900 MHz and a pulse repetition interval (PRI) of 4 μs, such that the total coherent processing interval (CPI) is 0.4 s. Each waveform has a 3-dB bandwidth of 50 MHz and 1 µs pulsewidth. Signal images produced by the AWG are suppressed by filtering with MiniCircuits SLP-1000+ lowpass filters. Each of these waveforms is then amplified by a separate MiniCircuits TVA-82-213 amplifier that produces the unintentional harmonic waveforms $s_{11}(t)$ and $s_{22}(t)$.

To emulate nonlinear scattering in a loopback configuration, the amplified outputs are combined using a MiniCircuits ZAPD-2-21-3W power combiner. The harmonic components of these signals then either remain unfiltered or are lowpass filtered by a MiniCircuits RDP-272+ absorptive diplexer. The resulting signal is injected into the nonlinear device under test (DUT), which in this context is a powered MiniCircuits ZFL-2000G+ wideband amplifier. At the receiver, the linear responses are highpass filtered using three MiniCircuits RDP-272+ absorptive diplexers in series such that nonlinearities within the receiver are mitigated. Without these filters, detection of the DUT nonlinear scattering would be limited by the second-order intermodulation and filter rejection of the receiver at the fundamental frequency.

Three different cases are evaluated. For Case 1 the transmitter harmonics are filtered and the DUT is present. Alternatively, for Case 2 the harmonics are not filtered and the DUT is removed. Finally, in Case 3 the harmonics are not filtered and the DUT is present. These different cases and their purposes are summarized in Table II.

The unintentional second-order harmonics produced by the TVA amplifiers (on "transmit") and the second-order intermodulation produced by the DUT each have a bandwidth of 100 MHz at a center frequency of 1800 MHz. Following the three diplexers in the "receive" chain, the harmonic and intermodulation components are bandpass filtered from 1750 MHz - 1850 MHz with a custom K&L Microwave filter and amplified with a MiniCircuits ZX60-33LN-S+. The I/Q data is captured at a center frequency of 1800 MHz and a sample rate of 200 MHz using a Rohde & Schwarz spectrum analyzer. This test setup is depicted in Figs. 4 and 5. Figure 6 illustrates the individual spectral components observed in Case 3 when both the harmonic and intermodulation waveforms are present.

TABLE II. EXPERIMENTAL EVALUATION OF SSPRINT NONLINEAR RADAR

Test Case	***Description***
Case 1	Harmonic waveforms suppressed and DUT is present: used to assess accuracy of the power series model of the intermodulation waveform
Case 2	Harmonic waveforms present and DUT removed: used to verify that modeled intermodulation waveform has low cross-correlation with harmonic waveforms
Case 3	Harmonic waveforms present and DUT is present: used to demonstrate that coherent averaging of FM noise based intermodulation waveforms provides significant gain relative to interference from harmonic waveforms

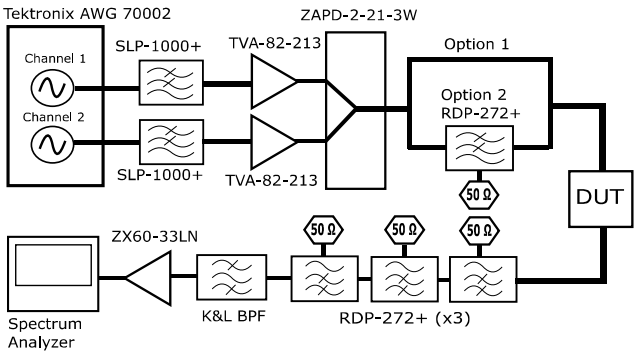

Fig. 4: Hardware setup for the SSPRInt loopback experiment

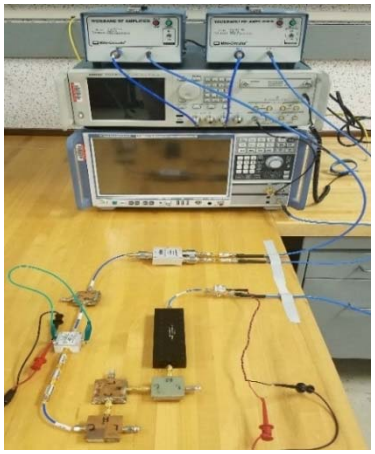

Fig. 5: Picture of hardware setup for Case 2

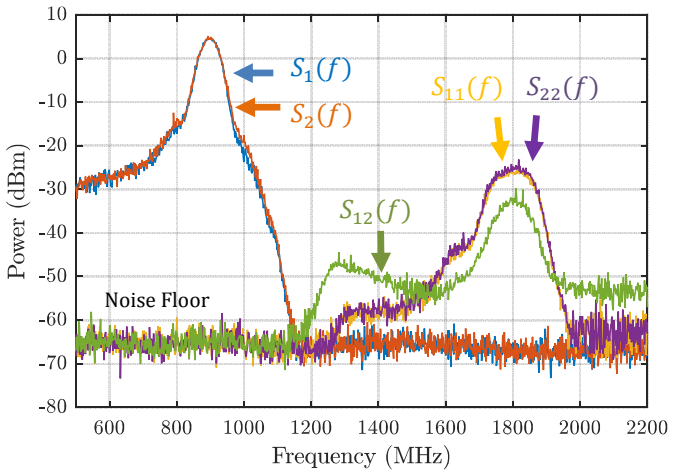

Fig. 6: Measured SSPRInt spectrum for Case 3

Case 1 is examined to determine the accuracy of the nonlinear power series approximation used to model the intermodulation waveform and that serves as the corresponding matched filter. By prior filtering, both $s_{11}(t)$ and $s_{22}(t)$ are attenuated below the noise floor. Figure 7 shows the normalized cross-correlation between the power series approximation of $s_{12}(t)$ and the measured data of Case 1 for a single pulse, 1000 coherently averaged pulses, and 100,000 coherently averaged pulses. Approximately 2 dB of mismatch loss is observed between the measured DUT response and the modeled power series approximation. As expected, the autocorrelation mainlobe experiences a coherent gain and the sidelobes are incoherently suppressed.

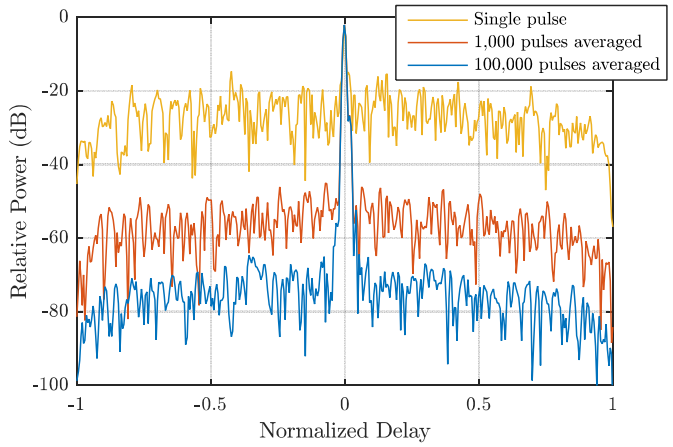

Fig. 7: Measured normalized nonlinear response using the power series approximation of $s_{12}(t)$ as matched filter for Case 1 for a single pulse, 1000 pulses averaged, and 100,000 pulses averaged

Case 2 is examined to verify that the power series approximation for $s_{12}(t)$ is uncorrelated with the unintentional "transmitter" harmonics generated by the TVA amplifier. Figure 8 shows the response of the DUT-free measurement to the power series modeled matched filter for $s_{12}(t)$, along with the result from Case 1 for comparison for 100,000 pulses coherently averaged. This result clearly shows that, with sufficiently unique waveforms, the harmonic responses can be made highly uncorrelated with the desired intermodulation response.

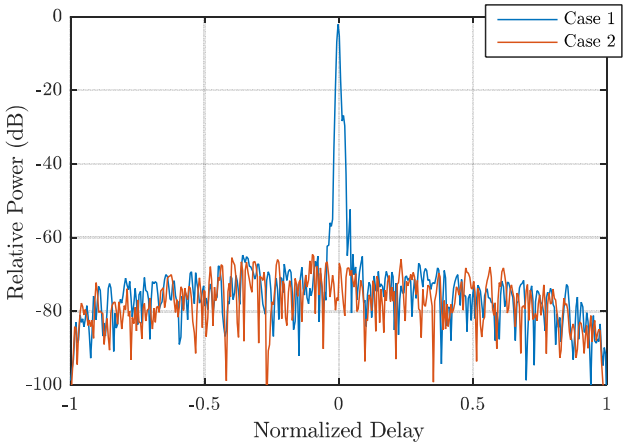

Fig. 8: DUT-free measurement match filtered with the power series approximation of the intermodulation waveform (Case 2) compared to Case 1 for 100,000 pulses averaged

Finally, the measured data in Case 3 possesses both intermodulation and harmonic waveforms. This measurement is again match filtered using the power series approximation of the intermodulation waveform. Here the intermodulation response is just barely visible for a single pulse. When more pulses are coherently combined, however, the intermodulation response is very clearly extracted from the harmonic interference. This result demonstrates that the SSPRInt method should be viable in practice.

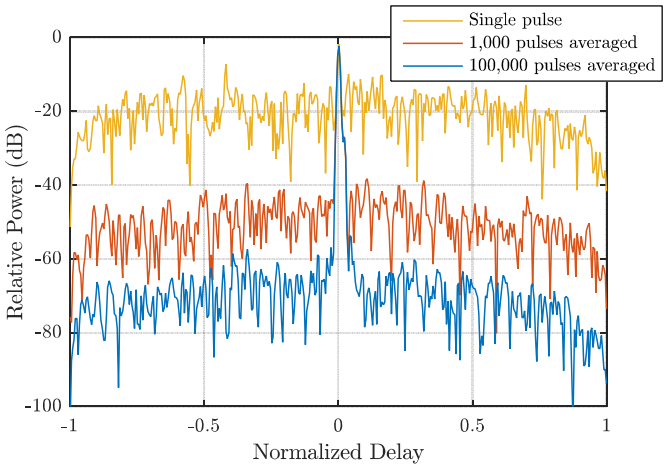

Fig. 9: Measurement containing both intermodulation and harmonic responses match filtered with the power series approximation of the intermodulation waveform (Case 3)

V. Conclusions

It has been demonstrated experimentally in loopback that the use of FM noise pulse pairs residing in the same spectrum can be used to elicit detectable intermodulation responses for nonlinear radar. The very high dimensionality of these

waveform sets enable the intermodulation response to be easily separable from harmonic responses in the same band that would otherwise mask its presence. These measurements also show that the power series approximation of the intermodulation waveform is a sufficiently good match with the measured version of this waveform.

REFERENCES

[1] R.O. Harger, "Harmonic radar systems for near-ground in-foliage nonlinear scatterers," *IEEE Trans. Aerospace & Electronic Systems*, vol. AES-12, no. 2, pp. 230-245, Mar. 1976.

[2] H.M. Aumann, N.W. Emanetoglu, "A wideband harmonic radar for tracking small wood frogs," *IEEE Radar Conf.*, Philadelphia, PA, May 2014.

[3] B. Kubina, J. Romeu, C. Mandel, M. Schüßler, R. Jakoby, "Design of a quasi-chipless harmonic radar sensor for ambient temperature sensing," *IEEE SENSORS*, Valencia, Spain, Nov. 2014.

[4] L. Chioukh, H. Boutayeb, D. Deslandes, K. Wu, "Noise and sensitivity of harmonic radar architecture for remote sensing and detection of vital signs," *IEEE Trans. Microwave Theory & Techniques*, vol. 62, no. 9, pp. 1847-1855, Sept. 2014.

[5] T.G. Leighton, D.C. Finfer, P.R. White, G.H. Chua, and J.K. Dix, **"**Clutter suppression and classification using Twin Inverted Pulse Sonar (TWIPS)," *Proc. Royal Society of London A*, vol. 466, pp. 3453-3478, Dec. 2010.

[6] T.G. Leighton, G.H. Chua, P.R. White, K.F. Tong, H.D. Griffiths, "Radar clutter suppression and target discrimination using twin inverted pulses," *Proc. Royal Society of London A*, vol. 469, Oct. 2013.

[7] G.J. Mazzaro, A.F. Martone, K.I. Ranney, R.M. Narayanan, "Nonlinear radar for finding RF electronics: system design and recent advancements," *IEEE Trans. Microwave Theory & Techniques*, vol. 65, no. 5, pp. 1716-1726, May 2017.

[8] K.A. Gallagher, G.J. Mazzaro, R.M. Narayanan, K.D. Sherbondy, A.F. Martone, "Automated cancellation of harmonics using feed-forward filter reflection for radar transmitter linearization," *Proc. SPIE 9077, Radar Sensor Technology XVIII*, May 2014.

[9] A.F. Martone, E.J. Delp, "Characterization of RF devices using two-tone probe signals," *IEEE Workshop on Statistical Signal Processing*, Madison, WI, Sept. 2007.

[10] G.J. Mazzaro, A.F. Martone, D.M. McNamara, "Detection of RF electronics by multitone harmonic radar," *IEEE Trans. Aerospace & Electronic Systems*, vol. 50, no. 1, pp. 477-490, Jan. 2014.

[11] G.J. Mazzaro, K.A. Gallagher, A.F. Martone, K.D. Sherbondy, R.M. Narayanan, "Short-range harmonic radar: chirp waveform, electronic targets," *Proc. SPIE 9461, Radar Sensor Technology XIX and Active and Passive Signatures VI*, May 2015.

[12] S.D. Blunt, E.L. Mokole, "An overview of radar waveform diversity," *IEEE Aerospace & Electronic Systems Mag.*, vol. 31, no. 11, pp. 2-42, Nov. 2016.

[13] M. Wicks, E. Mokole, S.D. Blunt, V. Amuso, R. Schneible, eds., *Principles of Waveform Diversity and Design*, SciTech Publishing, 2010.

[14] J. Jakabosky, S.D. Blunt, B. Himed, "Waveform design and receive processing for nonrecurrent nonlinear FMCW radar," *IEEE Intl. Radar Conf.*, Arlington, VA, May 2015.

[15] J. Jakabosky, S.D. Blunt, B. Himed, "Spectral-shape optimized FM noise radar for pulse agility," *IEEE Radar Conf.*, Philadelphia, PA, May 2016.

[16] J.A. Kosinski, W.D. Palmer, M.B. Steer, "Unified understanding of RF remote probing," *IEEE Sensors Journal*, vol. 11, no. 12, pp. 3055-3063, Dec. 2011.

[17] S.A. Maas, *Nonlinear Microwave Circuits*, Artech House, 1988.

[18] F. Giannini, *Nonlinear Microwave Circuit Design*, John Wiley & Sons, 2004.

[19] J.C. Pedro, N.B. Carvolho, *Intermodulation Distortion in Microwave and Wireless Circuits*, Artech House, 2003.

[20] S.R.J. Axelsson, "Noise radar using random phase and frequency modulation," *IEEE Trans. Geoscience & Electronic Systems*, vol. 42, no. 11, pp. 2370-2384, Nov. 2004.

[21] L. Pralon, B. Pompeo, J.M. Fortes, "Stochastic analysis of random frequency modulated waveforms for noise radar systems," *IEEE Trans. Aerospace & Electronic Systems*, vol. 51, no. 2, pp. 1447-1461, Apr. 2015.

[22] L. Pralon, G. Beltrao, B. Pompeo, M. Pralon, J.M. Fortes, "Near-thumbtack ambiguity function of random frequency modulated signals," *IEEE Radar Conf.*, Seattle, WA, May 2017.

[23] J. Jakabosky, S.D. Blunt, A. Martone, "Incorporating hopped spectral gaps into nonrecurrent nonlinear FMCW radar emissions," *IEEE Intl. Workshop Computational Advances in Multi-Sensor Adaptive Processing*, Cancun, Mexico, Dec. 2015.

[24] J. Jakabosky, B. Ravenscroft, S.D. Blunt, A. Martone, "Gapped spectrum shaping for tandem-hopped radar/communications & cognitive sensing," *IEEE Radar Conf.*, Philadelphia, PA, May 2016.

[25] B. Ravenscroft, P.M. McCormick, S.D. Blunt, J. Jakabosky, J.G. Metcalf, "Tandem-hopped OFDM communications in spectral gaps of FM noise radar," *IEEE Radar Conf.*, Seattle, WA, May 2017.

[26] B. Ravenscroft, S.D. Blunt, C. Allen, A. Martone, and K. Sherbondy, "Analysis of spectral notching in FM noise radar using measured interference," *IET Intl. Conf. Radar Systems*, Belfast, UK, Oct. 2017.

[27] J.W. Owen, B. Ravenscroft, B.H. Kirk, S.D. Blunt, C.T. Allen, A.F. Martone, K.D. Sherbondy, R.M. Narayanan, "Experimental demonstration of cognitive spectrum sensing & notching for radar," *IEEE Radar Conf.*, Oklahoma City, OK, Apr. 2018.

[28] G. Zook, P.M. McCormick, S.D. Blunt, C. Allen, J. Jakabosky, "Dual-polarized FM noise radar," *IET Intl. Conf. Radar Systems*, Belfast, UK, Oct. 2017.

[29] G. Zook, P. McCormick, S.D. Blunt, "Fixational eye movement radar: random spatial modulation," *IEEE Radar Conf.*, Oklahoma City, OK, Apr. 2018

[30] C.A. Mohr, P.M. McCormick, S.D. Blunt, "Optimized complementary waveform subsets within an FM noise radar CPI," *IEEE Radar Conf.*, Oklahoma City, OK, Apr. 2018.

[31] C.A. Mohr, P.M. McCormick, S.D. Blunt, C. Mott, "Spectrally-efficient FM noise radar waveforms optimized in the logarithmic domain," *IEEE Radar Conf.*, Oklahoma City, OK, Apr. 2018.

[32] S.D. Blunt, M. Cook, J. Jakabosky, J. de Graaf, E. Perrins, "Polyphase-coded FM (PCFM) radar waveforms, part I: implementation," *IEEE Trans. Aerospace & Electronic Systems*, vol. 50, no. 3, pp. 2218-2229, July 2014.